



# THE EFFECT OF VOIDS ON THE FLEXURAL FATIGUE PERFORMANCE OF UNIDIRECTIONAL CARBON FIBRE COMPOSITES

Mohamed A. Suhot\*, Alan R. Chambers\*

\*School of Engineering Sciences, University of Southampton, Highfield, Southampton. SO17 1BJ, UK

**Keywords:** voids, flexural fatigue, carbon fibre, acoustic emission, x-ray ctscan

## Abstract

*This study explores the effect of voids in the 1-6% range on the flexural fatigue properties of unidirectional carbon fibre reinforced epoxy polymer composites (CFRP) as used by the wind turbine industry. Samples with different void content were successfully obtained by varying the manufacturing process. Void content were acquired from three-point bending test samples and correlated with the three-point bending test results. There is a general trend of increasing fatigue strength with decreasing void content. Acoustic emission results show that the major failure is due to fibre breakage. Observation of damage using x-ray computed tomography shows failures that consist of crack under the roller and a separate delamination starting from voids.*

## 1 Introduction

The presence of defects can severely degrade the mechanical properties of composite materials and not surprisingly their effects have been extensively researched in recent years [1]. Voids are regarded as being particularly significant because they are inherent in any manufacturing process. Acceptable void levels vary from less than 1% in aerospace applications to in excess of 5% in automotive and marine applications.

There is a general agreement that the tensile (fibre dominated properties) are not significantly influenced by voids but it is well established that the matrix dominated properties such as compressive and flexural are significantly affected [2]. Ideally composites are not exposed to these loading regimes but in the case of wind turbines both compression and flexure are real issues.

Less attention has been given to the development of damage in composite laminates loaded in flexure due to the presence of both tensile and compressive stress in the material making it more difficult to interpret. In particular, studies on damage development for CFRP containing voids loaded in flexure are still not well explored.

The aims and objectives of this research are to develop an understanding of effect of voids on the fatigue behaviour of unidirectional carbon/epoxy composites.

## 2. Background

For CFRP, the tensile fatigue resistance at stresses below 80% of the static strength is excellent. However, in flexural fatigue, damage occurs at smaller loads and after a fewer cycles [3]. Flexural fatigue loading was reported to have a more serious effect on the fatigue resistance of the composite compared with uniaxial loading because it places a more severe stress on the matrix of the composite.

Several researchers have described how unidirectional CFRP failed from flexural fatigue damage. Croman [4] observed that fatigue failure initiation was by compression failure in the vicinity of the loading nose. This damage increased in length toward the mid-plane. With increasing cycles, delaminations to the right and left appeared and grew until the specimen finally failed into two pieces via tensile breaking of the fibres on the tensile side of the specimens. Failure started at compression side due to the downward thrust of the point loading that subjected the uppermost fibres to longitudinal compression and lateral thrust. The fibres buckled and failed at the same time resulting in the sudden appearance of compression side cracks.

There are several reasons for the decrease of strength due to the presence of voids, including voids acting as a break in fibre-matrix adhesion [2], shearing due to the presence of voids in fibre/matrix interface and resin [5], voids reducing the cross-sectional area and acting as failure initiator [6] and a variation of a notched strength criterion [7]. In a review of bending tests, Mullin and Knoell [8] discussed the effects of specimen flaw such as voids on flexural strength. The maximum flexural stress location is at the outermost layers of the laminate and the maximum shear stress is at the vertical plane under the loading roll. Therefore a single flaw at these locations could diminish the overall flexural strength.

### 3. Experimental procedures

#### 3.1 Materials

Both SPRINT<sup>\*</sup> and prepreg were used to produce four ply unidirectional carbon/epoxy composites. SPRINT materials consist of a layer of fibre reinforcement on each side of a precast, precatalysed resin film, with a light tack film on one face. SPRINT is different from the usual prepreps, in the sense that its fibres stay dry and unimpregnated by the resin until the curing process [9]. For the prepreg materials, the base material is a carbon/epoxy prepreg by SP Systems, made of 500g/m<sup>2</sup> of unidirectional carbon fibre. All the laminates were manufactured by vacuum bagging process.

The primary objective of this work is to investigate the effect of voids on the flexural fatigue performance. In order to achieve a range of voids, SPRINT laminates were produced using vacuum pressures of 70%, 80%, 90% and 100% of the manufacturer's recommended vacuum pressure (70% vacuum is an inferior to 100% vacuum). For the prepreg laminates, the difference in quality was achieved by debaulking and non-debaulking.

#### 3.2 Image analysis

To determine the quality of the laminate, void contents were measured using computerized image analysis. Void content measurements were made on previously tested flexural fatigue specimens to gain a void content representative of the material in the failure zone. Thus image analysis was conducted 30

mm away from the failure point along the axis perpendicular to the direction of the fibre orientation. Next the statistical average of void percentages in the processed images was taken as equal to the void volume percentage. This method is thus far considered among the most precise for measuring the void content [10].

Carefully prepared specimens were placed under an optical Olympus BH-2 microscope interfaced to a PC based computer using a DVC digital video camera module. Voids in the image in the optical microscope analysis were separated from the background (resin and fibres) by adjusting the light intensity of the microscope until only the voids were highlighted. The images were fed to the computer using XCap image analysis software.

In this study, a Windows-based tessellation module developed by Boselli [11] called Tessellation Analysis Program (TAP), was used to study the voids characteristics. Using TAP, the voids were highlighted by thresholding the image. The threshold level was set in such a way that resin and fibres appeared white while voids were red. Further manual editing may be needed to select or deselect areas in the image which could be voids or not. The software then calculates the percentage of red area and hence the void fraction. The sequence is summarized in Figure 1(a)-(c).

Each sample were analysed at a magnification of 100x using 5 images taken at 2.5 mm intervals across the specimen. On the basis of previous work, five images per specimen was considered optimal. The average percentages of void content for the specimens were taken as the void content percentage for the laminate. The voids were also classified into four different void types depending on the void size,  $V$ : type 1 ( $8 \times 10^{-6} < V < 0.004 \text{ mm}^2$ ), type 2 ( $0.004 < V < 0.01 \text{ mm}^2$ ), type 3 ( $0.01 < V < 0.03 \text{ mm}^2$ ) and type 4 ( $V > 0.03 \text{ mm}^2$ ).

#### 3.3 X-ray computed tomography

X-ray computed tomography is a non-destructive technique for obtaining images of internal microstructure of material. It has been originally used for biomedical purposes. The field was pioneered by Feldkamp et al. [12]. In X-ray computed tomography, an x-ray source scans the object that is placed between the source and a detector. The resulted transmissions of x-rays are recorded on a detector that measures the different intensities of the attenuated x-rays. The specimen is rotated for a fixed rotation step. A 3D representation

\* SP Systems trademark

of an object is obtained by stacking computed tomography (CT) slices of the object in many parallel planes inside the object.

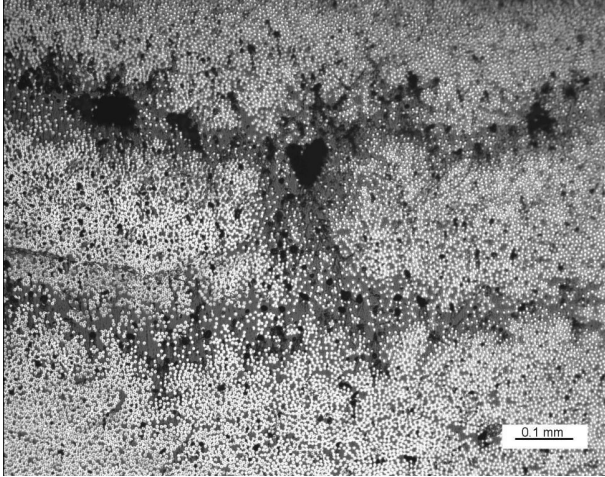


Fig. 1(a). Original image of laminate



Fig. 1(b). Image after intensity adjusting, leaving black area as voids while resin and fibres are white



Fig. 1(c). Image after thresholding. The software then calculates the percentage of the red area.

Three point bend specimens were scanned to identify voids prior to mechanical testing. Subsequently, selected specimens were examined at various stages in their fatigue life by periodically stopping the testing, re-examining to identify the effect of voids on fatigue damage/mechanism and continuing the testing to failure.

X-ray micro CT images were acquired using X-TEK Benchtop CT 160Xi machine. It is a benchtop type machine which has a resolution down to 5  $\mu\text{m}$  focal spot reflection target and an x-ray source which operate at 25-160 kV and 0-1000  $\mu\text{A}$ . The scans in this study were conducted with x-rays at a voltage of 45 kV and a current of 100  $\mu\text{A}$ . The three-dimensional reconstruction is done using CT-Pro and visualization and analysis is done using VGStudiomax.

### 3.4 Acoustic emission

Acoustic emission (AE) has been established as a technique to study the damage development and the structural integrity of composite materials. Low-amplitude AE signal is commonly attributed to matrix cracking, whereas the high-amplitude AE signal is due to fibre breaking [13]. In this work, one piezoelectric sensor was mounted using a hot glue gun on the underside of the specimens directly under the loading roller.

### 3.5 Mechanical tests

#### 3.5.1 Static tests

Prior to fatigue testing, the static flexural strength of a material was established in accordance with ASTM standard D790 [14]. The span-to-depth ratio was 16:1. The tests were performed using an Instron 8872 mechanical testing machine under load control. The crosshead speed was calculated using procedure A from the standard which was 0.85 mm/min (calculated from the specimen and setup geometry).

For each specimen, the maximum loads were determined from the data logger. Using the maximum load, the maximum flexural stresses for each specimen were calculated using the relation:

$$\sigma_{\max} = \frac{3PL}{2bd^2}$$

The maximum flexural stresses from the specimens were averaged (12 specimens) and used to calculate the maximum load for the fatigue test.

3.5.2 Fatigue tests

Fatigue tests were performed on specimens identical to those used in the static tests. The ratio of minimum load,  $P_{min}$  to maximum load,  $P_{max}$  ( $R$  ratio) was 0.1. The cycle rate was 4 Hz to avoid the effects of heating of the resin system. A sinusoidal waveform was used. The tests were load-controlled, and therefore the maximum and minimum load was kept constant through the fatigue life of the specimens. Tests were terminated at 2 mm specimen deflection.

4. Results and discussions

4.1 Void content

The average of void content for each vacuum pressure is shown in Table 1. It is clear from the table that the use of higher vacuum pressure reduces the void content in the laminates. This reduction in void content can be explained by considering the establishment of a high local pressure that minimize individual bubbles and also cause small voids to dissolve into the resin [2].

For the debulked prepreg laminate the void content was found to be 3.6% while for the non-debulked laminate the void content was 6.8%. Larger voids were found in both prepreg laminates compared with the SPRINT materials at any vacuum pressure. The inferior quality of the non-debulked prepreg laminate shows the importance of debulking in the production of high quality laminates.

Table 1. Void content of the different vacuum pressure panels

Vacuum pressure (%)	Average void content (%)
100	1.63
90	2.51
80	2.71
70	2.89

4.2 Effect of voids on three-point bending fatigue strength

The effect of void content on three-point bending fatigue strength is shown in Figure 2. There is a general trend of increasing fatigue strength with decreasing void content and the sprint and prepreg samples fit on the same trend line. In order to establish the effect of void size, the normalized number density of types 1, 2, 3 and 4 voids was plotted as a function of vacuum pressure/void

content (Figure 3). Types 1, 2 and 3 are largely independent of vacuum pressure but type 4 increases as vacuum decreases/void content increases. It can therefore be concluded that for SPRINT laminates with voids in the 1–4% range, the reduction in fatigue performance with increasing void content is caused by type 4 voids (area > 0.03 mm<sup>2</sup>).

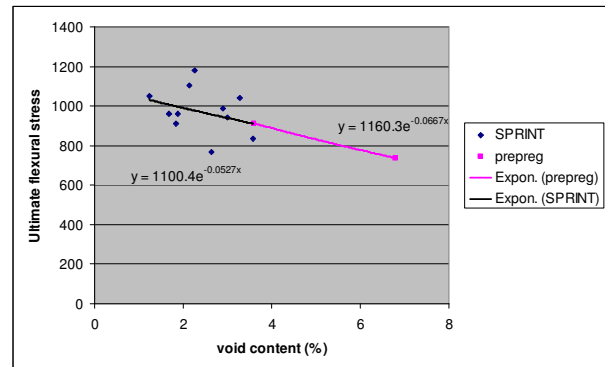


Fig. 2. Failure cycles vs. void content using 90% of maximum stress.

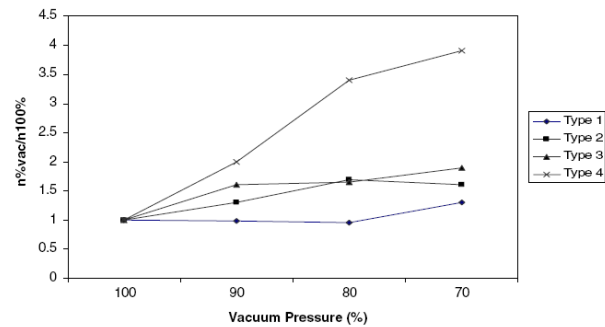


Fig. 3. Normalised void number density as a function of void content

4.3 Fatigue damage accumulation

The fatigue damage accumulation was studied by monitoring the deflection of the samples during the fatigue tests. The tests were performed under load control and the specimens' degradation was monitored by the deflection measurements. The result shown in the graph (Figure 4) is the relative deflection (%), i.e., the deflection at first cycle divided by deflection at cycle  $N$ , as a function of the normalized number of cycles (%). It can be ascertained from this curves the percentage of life at which fatigue degradation occurred.

The 100% vacuum specimen curve, which is representative of a high quality specimen, shows the typical three stages of damage development of continuous fibre composites [15]. The first stage is short lived but shows a rapid increase of deflection

which can be regarded as the fatigue damage initiation stage. This is followed by the second stage which relates approximately to a plateau, which continues over an important period of the fatigue life. In the third stage, the deflection increases quickly towards fatigue failure. This curve can be termed as 'sudden death' behaviour where the deflection does not increase until impending failure.

For the 70% vacuum SPRINT laminate, damage accumulates steadily throughout the fatigue life. Test specimens which demonstrate this type of behaviour would invariably have a shorter life under the same fatigue conditions.

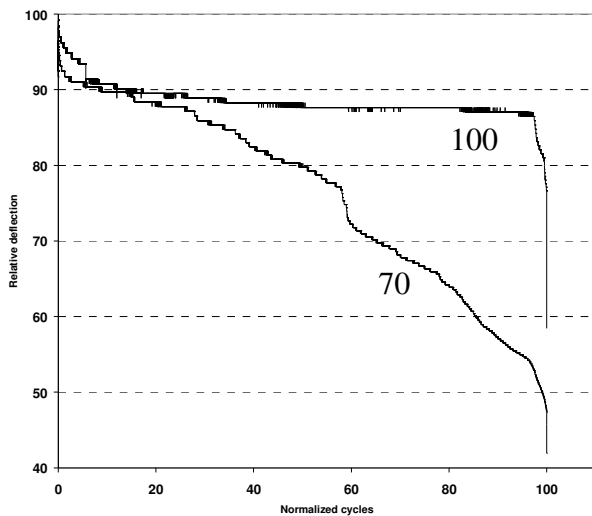


Fig. 4. Three-point bending fatigue stiffness degradation for low void content (100) and high void content (70)

#### 4.4 X-ray tomography results

Figure 5 shows the x-ray tomography result of seven static and fatigue test specimens and one reference material. It is a typical result of an x-ray tomography showing a 3D image and three image views of the specimens. The result provides a clear contrast between voids and cracks and the surrounding area which is fibre and matrix. The contrast between fibre and matrix however is not very clear.

The effect of voids on static and flexural fatigue damage was studied. Typical results for static test are shown in Table 2 for longitudinal view. Specimen 5.8, which was stopped after the first load drop, demonstrates early stage failure. It can be seen that a crack is starting at the surface of the specimen under the roller. Specimen 6.2 was tested to failure. It can be seen that the crack under the roller for this specimen is catastrophic. A large

void is visible before loading. This void is seen to initiate a longitudinal crack and also connect to the crack which is developing under the roller.

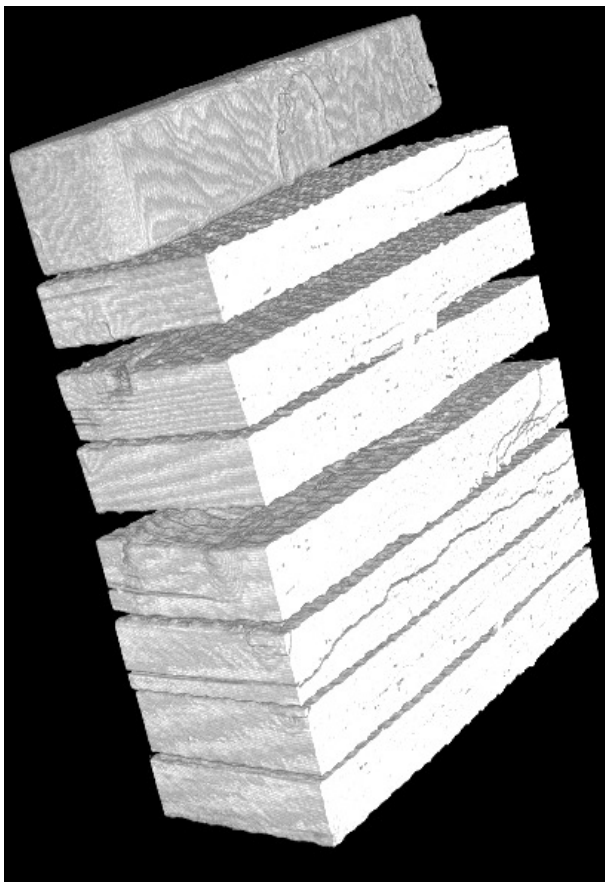
Typical fatigue damage sequence is shown in Table 3. Specimen 6.5 was tested until 1 mm deflection and specimen 6.3 until 2 mm deflection which was the failure condition. At 2 mm deflection, a crack under the roller has developed and a crack initiating at a void can be seen. Note that, for static specimen, crack under the roller appeared at the start of the test.

The cross sectional views of static test and fatigue test specimens are shown in Figure 6 to 9. For specimen 5.8 where the test was stopped after load start to drop, it can be seen that there is initial damage starting from the surface under the roller propagating towards the middle of the specimen and propagating to the left and to the right of the specimen (Figure 6). This crack is seen to connect to voids.

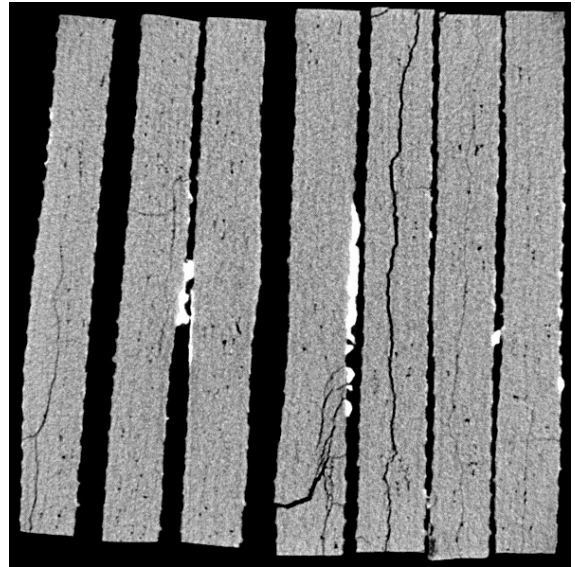
For specimen 6.2 (Figure 7) where the static test was taken until failure, a crack is seen to initiate from a void and propagate to the edge of the specimen. The absence of a crack under the roller indicates that this is not necessarily the initiator of final failure.

For fatigue test, Figure 8 shows specimen 6.5 where fatigue test was stopped when deflection reached 1.0 mm. It can be seen that a crack is initiating mid - plane and is propagating through voids. However there is also a crack that does not run through voids. Specimen 6.3 where was tested until 2.0 mm deflection is shown in Figure 9. It can be seen that there is a crack from under the roller which is not shown in specimen 6.5. There is also a crack starting from a void. The figure shows that for fatigue failure, the major mid-plane crack has run through the cross section.

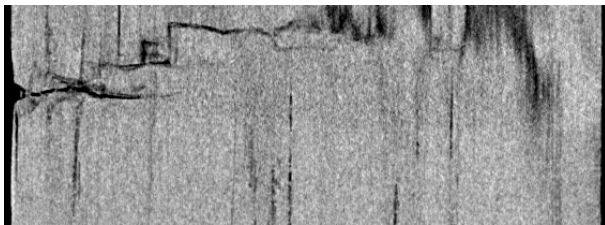
Sectioning the specimen longitudinally enabled the specimen to be placed nearer to the x-ray source. This improved the contrast and enabled the resin rich areas to be identified (Figure 10). The larger voids were found to be cylindrical as reported by other researchers [1].



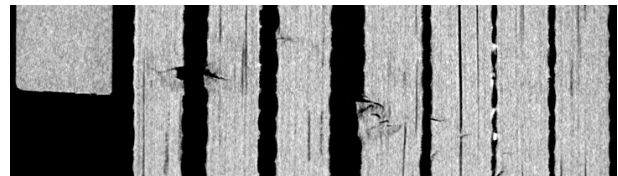
(a)



(b)



(c)



(d)

Fig. 5. X-ray tomography results of the specimens. (a) 3D image (b) cross-sections normal to the fibres, (c) face side of one specimen (d) longitudinal side view of the specimens.

**THE EFFECT OF VOIDS ON THE FLEXURAL FATIGUE PERFORMANCE OF UNIDIRECTIONAL CARBON FIBRE COMPOSITES**

Table 2. X-ray tomography images of longitudinal side view before and after loading – static test

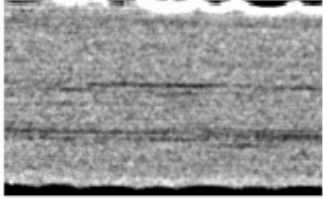
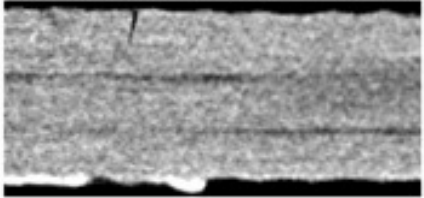
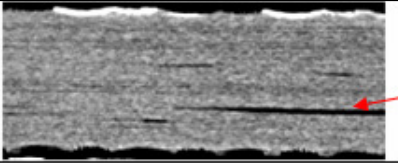
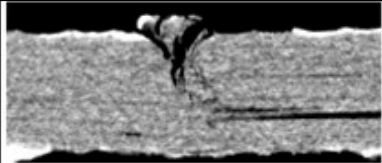
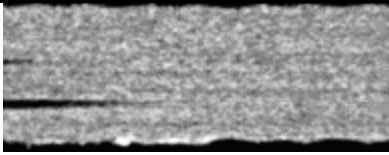
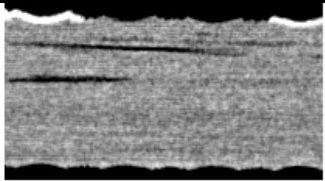
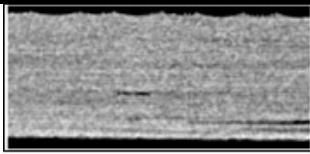
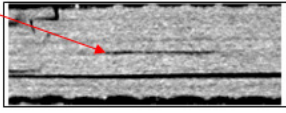
	Before loading	After loading
5.8 static starting		
6.2 static failure	 void	

Table 3. X-ray tomography images of longitudinal side view before and after loading – fatigue test

	Before loading	After loading
6.5 fatigue – deflection 1mm		
6.3 fatigue – deflection 2 mm		 A crack starting from a void

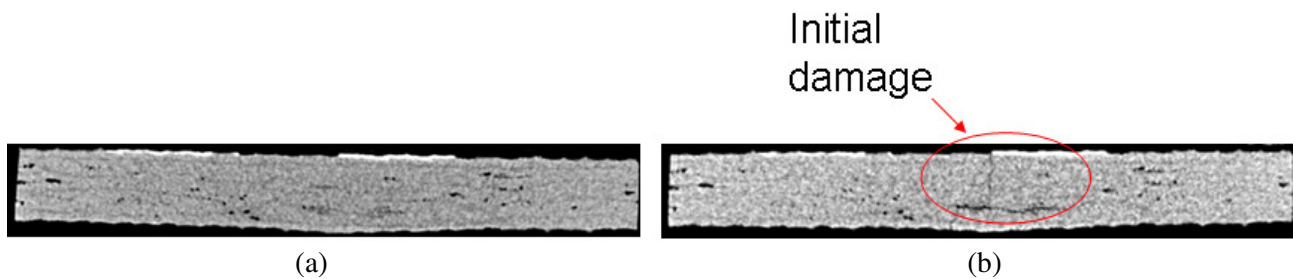


Fig. 6. X-ray tomography images of cross-sectional view for specimen 5.8 (a) before and (b) after loading



Fig. 7. X-ray tomography images of cross-sectional view for specimen 6.2 (a) before and (b) after loading

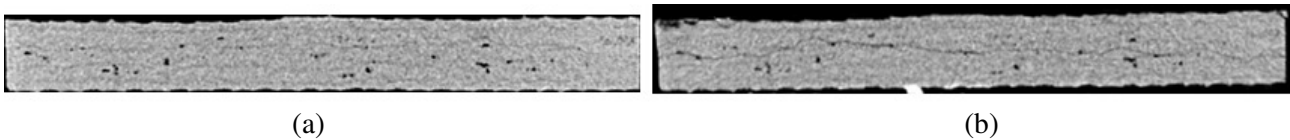


Fig. 8. X-ray tomography images of cross-sectional view for specimen 6.5 (a) before and (b) after loading.

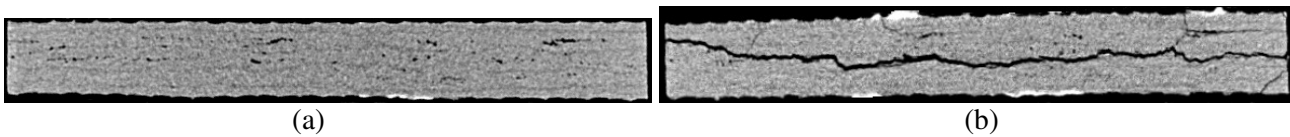


Fig. 9. X-ray tomography images of cross-sectional view for specimen 6.3 (a) before and (b) after loading

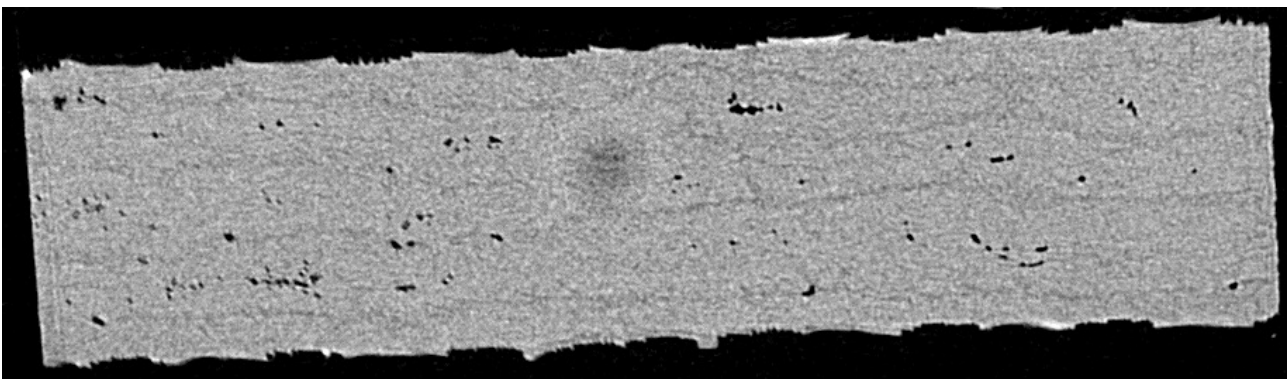


Fig. 10. Smaller specimen produce better image which shows resin rich area in the sample.

#### 4.5 Fatigue mechanism

Failure consists of a crack under the roller and delamination either to the left or to the right of the specimen, typically shown in Figure 5(d). This is because the compressive strength is much lower than tensile strength [16]. Kinking is observed in the compression area beneath the loading rollers as were observed by Parry and Wronski [17] (Figure 11). A typical AE result from the fatigue test is shown in Figure 12. It can be seen that the sudden increase in deflection corresponds to a high amplitude event which is fibre breakage. The AE result shows that the major failure during the loading is fibre breakage.

Results from x-ray tomography indicate that the crack under the roller is not connected to the delamination. Two types of failure can be assumed from the results. The crack from under the roller is due to the downward thrust of the roller and voids are not directly responsible for this failure. However, the delamination failure is due to defects inside the sample which in this case is due to voids.

The fatigue samples rarely broke into two pieces by delamination. In general, delamination failure ended close to one of the two bottom rollers, and only in a few specimens on both sides of the loading roller. In some specimens the crack continues up to the end of the specimen.

# THE EFFECT OF VOIDS ON THE FLEXURAL FATIGUE PERFORMANCE OF UNIDIRECTIONAL CARBON FIBRE COMPOSITES

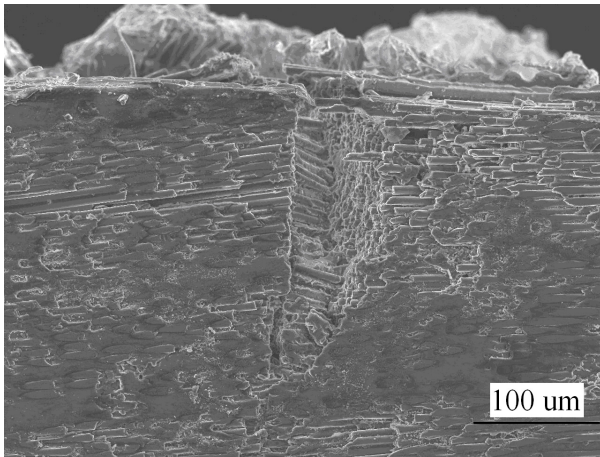


Fig. 11. Side view showing initial failure event.

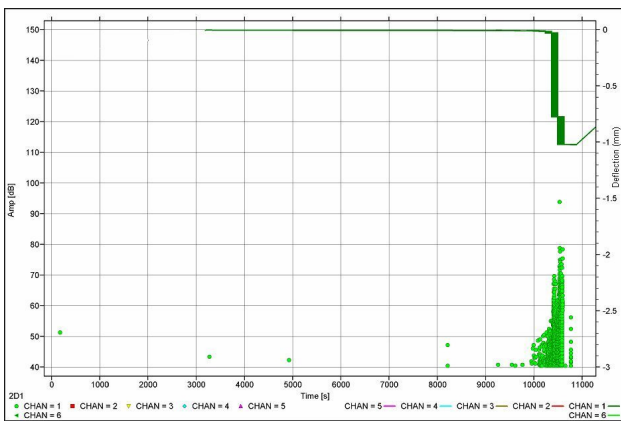


Fig. 12. Typical AE result from fatigue test.

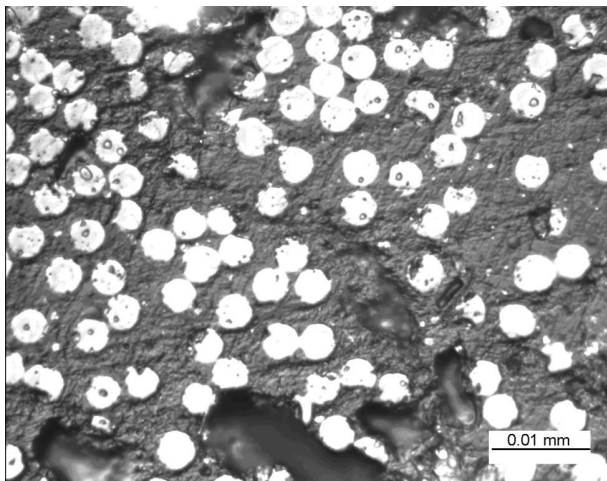


Fig. 13. Microstructures of 100% vacuum pressure samples with 1000X magnification

Microstructures of specimens 100-3.2 studied using 1000X magnification (Figure 13) shows small cracks initiating from voids and connecting to other

voids. Based on the figure it could be said that voids may act as initiator of cracks in composites and helps in the propagation of cracks.

## 5 Conclusions

Varying manufacturing process has presented various void content from 1% to 6% assessed from microscopic image analysis. Flexural fatigue experiments were conducted to investigate how the voids affect the mechanical response of unidirectional CFRP samples. A general trend of decreasing fatigue strength with increasing void content is obtained. Three-dimensional feature of void investigated using x-ray tomography has confirmed previous study that voids is cylindrical. Microscopic analysis proved the existence of crack initiation from voids and propagation to other voids. However results from x-ray tomography studies show that not all voids are involved in crack propagation.

## References

- [1] Talreja R., 'Effects of manufacturing induced defects on composite damage and failure', *Proceedings of the 27<sup>th</sup> Riso International Symposium on Material Science*, Roskilde, Denmark, 2006
- [2] Olivier P., Cottu J. P. and Ferret B. 'Effects of cure cycle pressure and voids on some mechanical properties of carbon/epoxy laminates', *Composites*, 26, 509-515, (1995)
- [3] Harris B., 'The nature and properties of carbon fibres and their composites', In: Marcus L, editor. *Carbon Fibres in Engineering*. London. McGraw-Hill, 1973. p. 1-45
- [4] Croman R. B., 'Flex fatigue of AS-4 graphite reinforced thermoplastics', *Proceedings of the Sixth International Conference on Composite Materials combined with the Second European Conference on Composite Materials*, London, UK, 20-24 July 1987, 4.76-4.88.
- [5] Jeong H., 'Effects of voids on the mechanical strength and ultrasonic attenuation of laminated composites', *Journal of Composite Materials*, 31, 276-292, (1997)
- [6] Wisnom M. R., Reynolds T., Gwilliam N., 'Reduction in interlaminar shear strength by discrete and distributed voids', *Composites Science and Technology*, 56, 93-101, (1996)
- [7] Almeida S. F. M. and Neto Z. S. N., 'Effect of void content on the strength of composite laminates', *Composite structures*, 28, 139-148, (1994)
- [8] Mullin J. V., Knoell A. C., 'Basic concepts in composite beam testing', *Materials Research and Standards*, 10, 16-20, (1970)

- [9] Overview of SPRINT® - SP Resin Infusion Technology, [CD-ROM], The SP Systems RefNet™ CD-ROM, Version 7.2, Newport, Isle of Wight, SP Systems, (2002)
- [10] Ghiorse S. R., 'Effect of void content on the mechanical properties of carbon/epoxy laminates', SAMPE Quarterly, 24, 54-59, (1993)
- [11] Boselli, J., 'Quantification of the effects of reinforcement distribution and morphology on fatigue in Al-SiC composites, PhD Thesis, Faculty of Engineering, University of Southampton, (1999)
- [12] Feldkamp L., Goldstein S. and Parfitt A., 'The direct examination of three-dimensional bone architecture in vitro by computed tomography', The Journal of Bone and Mineral Research, 4, 3-11, (1989)
- [13] Kim, S.-T. and Lee, Y.-T., 'Characteristics of damage and fracture process of carbon fiber reinforced plastic under loading-unloading test by using AE method', Materials Science & Engineering, v234-236, p322-6, (1997)
- [14] Standard test methods for flexural properties of unreinforced and reinforced plastics and electrical insulating materials (metric). Philadelphia, PA,: American Society for Testing and Materials, 1990 (ASTM D790)
- [15] Van Paepegem W. and Degrieck J., 'A new coupled approach of residual stiffness and strength for fatigue of fibre-reinforced composites', International Journal of Fatigue, 24, 747-762, (2002)
- [16] Wisnom M., 'The flexural strength of unidirectional carbon fibre-epoxy', *Developments in the Science and Technology of Composite Materials, Fifth European Conference on Composite Materials*, Bordeaux, France, 7-10 April, 1992, 165-170
- [17] Parry T. V. and Wronski A. S., 'Kinking and Tensile, Compressive and Interlaminar Shear Failure in Carbon-fibre-reinforced Plastics Beams Tested in Flexure', Journal of Materials Science, 16, 439-450, (1981)